HHS Public Access

Author manuscript

Neurobiol Dis. Author manuscript; available in PMC 2018 October 01.

Published in final edited form as:

Neurobiol Dis. 2017 October ; 106: 191–204. doi:10.1016/j.nbd.2017.07.007.

Nortriptyline inhibits aggregation and neurotoxicity of alpha-synuclein by enhancing reconfiguration of the monomeric form

Timothy J. Collier[1,2,*], **Kinshuk R. Srivastava**[3,#], **Craig Justman**[4], **Tom Grammatopoulous**[5], **Birgit Hutter-Paier**[6], **Manuela Prokesch**[6], **Daniel Havas**[6], **Jean-Christophe Rochet**[7], **Fang Liu**[7], **Kevin Jock**[3], **Patrícia de Oliveira**[3], **Georgia L. Stirtz**[8], **Ulf Dettmer**[8], **Caryl E. Sortwell**[1,2], **Mel B. Feany**[9], **Peter Lansbury**[4,8], **Lisa Lapidus**[3,+], and **Katrina L. Paumier**[10,+]

[1]Department of Translational Science and Molecular Medicine, Michigan State University, Grand Rapids, MI USA

[2]Mercy Health Hauenstein Neuroscience Center, Grand Rapids, MI USA

[3]Department of Physics and Astronomy, Michigan State University, East Lansing, MI USA

[4]Lysosomal Therapeutics, Inc., Cambridge, MA, USA

[5]BioEnergetics, Boston, MA, USA

[6]QPS Research, Graz, Austria

[7]Department of Medicinal Chemistry and Molecular Pharmacology, Purdue University, West Lafayette, IN, USA

[8]Ann Romney Center for Neurologic Diseases, Brigham and Women's Hospital and Harvard Medical School, Boston, MA, USA

[9]Department of Pathology, Brigham and Women's Hospital, Boston, MA, USA

[10]Department of Neurology, Washington University, Saint Louis, MO, USA

Abstract

The pathology of Parkinson's disease and other synucleinopathies is characterized by the formation of intracellular inclusions comprised primarily of misfolded, fibrillar α-synuclein (α-syn). One strategy to slow disease progression is to prevent the misfolding and aggregation of its native monomeric form. Here we present findings that support the contention that the tricyclic antidepressant compound nortriptyline (NOR) has disease-modifying potential for synucleinopathies. Findings from *in vitro* aggregation and kinetics assays support the view that

[*]Corresponding author: Timothy J. Collier, Michigan State University/College of Human Medicine, Department of Translational Science & Molecular Medicine, 333 Bostwick Ave. NE, Grand Rapids, MI 49503, timothy.collier@hc.msu.edu, Telephone: 616-234-0953.

[#]Co-first author designation

[+]Co-senior author designation

Conflict of Interest: The authors declare no competing financial interests.

NOR inhibits aggregation of α-syn by directly binding to the soluble, monomeric form, and by enhancing reconfiguration of the monomer, inhibits formation of toxic conformations of the protein. We go on to demonstrate that NOR inhibits the accumulation, aggregation and neurotoxicity of α-syn in multiple cell and animal models. These findings suggest that NOR, a compound with established safety and efficacy for treatment of depression, may slow progression of α-syn pathology by directly binding to soluble, native, α-syn, thereby inhibiting pathological aggregation and preserving its normal functions.

Keywords

alpha-synuclein; Parkinson's disease; biophysics; pre-formed fibrils; transgenic mouse; transgenic *Drosophila*; antidepressants; nortriptyline

Introduction

Parkinson's disease (PD) is a member of a class of neurodegenerative syndromes termed synucleinopathies, characterized by abnormal accumulations of the protein alpha-synuclein (α-syn) within selectively vulnerable neurons or glial cells (McCann et al., 2014). These syndromes are relentlessly progressive with no disease modifying therapy available at present. α-Syn is widely distributed in the central nervous system, representing approximately 1% of all cytosolic protein in brain (Iwai et al., 1995). In its native state, α-syn is mainly localized to synaptic terminals and the nucleus (Iwai et al., 1995; Yu et al., 2007). Soluble, monomeric α-syn is an intrinsically disordered protein (Theillet et al., 2016). Several membrane-bound helical conformations have been identified, ranging from monomeric to multimeric (Snead and Eliezer, 2014). Membrane conformers are in equilibrium with the cytosolic, disordered monomer (Burré et al., 2015). Although the normal function of α-syn is not fully understood, it is involved in synaptic plasticity (George et al., 1995; Watson et al., 2009), vesicle pool maintenance (Murphy et al., 2000), and neurotransmitter release (Abeliovich et al., 2000; Burré et al., 2010, 2014). Under conditions in which α-syn homeostasis is perturbed, the protein misfolds and forms insoluble amyloid fibrils associated with neuropathology. In PD, α-syn is the primary component of intracellular Lewy body inclusions diagnostic for the disease (Spillantini et al., 1997). Genetic forms of PD have been linked to multiplications and mutations of the α-syn gene locus, further implicating α-syn in the pathogenesis of PD (Polymeropoulos et al., 1997; Ibáñez et al., 2004; Singleton et al., 2003; Simón-Sánchez et al., 2009).

One reasonable approach to therapy for synucleinopathies is to inhibit accumulation and aggregation of α-syn while maintaining its native states and normal functions. Many strategies have used fibril formation as the indicator that inhibition has been achieved. However, evidence supports the contention that fibrilization is a multi-step process and that fibrils are not in themselves toxic (Chiti and Dobson, 2006; Lashuel et al., 2013). While prior studies indicate that the process of aggregation initiates from the disordered monomer (Burré et al., 2015; Dettmer et al., 2015), it is thought that lower molecular weight oligomers are likely the toxic species (Winner et al., 2011; Pinotsi et al., 2016). Therefore, inhibition of

the formation of toxic α-syn conformations must occur at the earliest stages, perhaps at the monomer level.

We report here that the tricyclic antidepressant drug nortriptyline (NOR) inhibits aggregation of α-syn through interaction with the monomeric form. We provide evidence from *in vitro* kinetics assays that NOR binds directly to α-syn and affects the ensemble of unfolded conformations to promote more expanded structures that are more rapidly diffusing, making formation of the first oligomeric dimer less likely. Furthermore, we demonstrate that NOR inhibits aggregation and neurotoxicity of α-syn in cell and animal models. Taken together, this suggests that NOR has potential as a disease-modifying intervention for synucleinopathies such as PD and provides a pharmacoepidemiologic template for development of novel therapeutic agents.

Materials and Methods

α-Syn aggregation assays

Preparation of human wild-type α-syn—Recombinant α-syn protein for aggregation assays was expressed in E. Coli and purified to > 95% purity. Expression and purification were performed by The University of Iowa Center for Biocatalysis and Bioprocessing using a previously published protocol with slight modifications (Conway et al., 1998). Briefly, cell pellets were resuspended in Buffer A (10mM Tris-HCl, pH 7.4) with E-64c protease inhibitor, and then lysed by passing through a microfluidizer. Proteins precipitated by addition of 25% ammonium sulfate were resuspended in Buffer A with E-64c, then ultrafiltered through a 100 kDa MWCO filter. After buffer exchange via diafiltration, proteins were loaded on DEAE-650S column and eluted with a gradient of NaCl in Buffer A. Fractions were analyzed by SDS-PAGE for the presence of α-syn. Pooled fractions were buffer exchanged into 50mM ammonium bicarbonate, then lyophilized.

Preparation of α-syn-fluorophore conjugate—A solution of recombinant wild-type α-syn in PBS was dialyzed against PBS, pH 7.0 overnight. Dialyzate was ultrafiltered through a 100 kDa MWCO membrane. The protein concentration was determined by absorbance at 280nm, then diluted to 500μM with PBS. One vial of Alexa Fluor 594 carboxylic acid, succinimidyl ester (Alexa Fluor 594 Protein Labeling kit, A10239) was resuspended in 50μl DMSO and immediately added to the stirring α-syn solution. The reaction proceeded in the dark at room temperature for 1.5 hours. The complete reaction mixture was applied directly to a 3ml Sephadex G-75 column equilibrated in 20mM Bis-Tris Propane, pH 6.5, 100mM LiCl. Fractions containing Alexa Fluor 594 α-syn conjugate were identified by fluorescence intensity and fluorescence polarization in a Molecular Probes Analyst using a 546nm band-pass filter for excitation, a 595nm dichroic mirror, and a 620nm band-pass emission filter.

Aggregation assays—A solution of recombinant wild-type α-syn in 20mM Bis-Tris Propane pH 6.5, 100mM LiCl was ultrafiltered through a 100kDa MWCO membrane. Concentration was determined by absorbance at 280nm. Aggregation reactions were performed with 70μM human α-syn and 200nM AXS in 20mM Bis-Tris Propane pH 6.5, 100mM LiCl in a total volume of 750μl in a 1.5ml polypropylene tube. Triplicate tubes were

treated with either nortriptyline (20x stock in DMSO) or 5% DMSO. Aggregation was performed at 37°C with gentle agitation via rotation in a tissue culture roller at approximately 60 RPM. To monitor aggregation progression, tubes were vortexed for 3 seconds, then aliquots were removed for analysis. For fluorescence polarization, 5μl of aggregation reaction was diluted with 45μl 50mM Tris-HCl, pH 7.4 in a black 384 well plate (Greiner Fluotrac). Fluorescence polarization was read on a Molecular Devices Analyst using a 546nm band-pass filter for excitation, a 595nm dichroic mirror, and a 620nm band-pass emission filter. Treatment groups were compared to DMSO alone with a two-tailed t-test using GraphPad Prism 6.0 (La Jolla, CA). For loss of monomer experiments, 20μl aliquots of reaction were centrifuged (14,000 g × 15′) to remove fibrillar material, then 5μl of supernatant was diluted with 50μl of mobile phase (20mM Bis-Tris propane, 100mM LiCl, pH 7.4). The diluted solution was passed through a 2ml Shodex KW-G gel filtration column with prefilter, separating monomer from higher order multimers. The elute was monitored by absorbance at 276nm and peak area for monomer was quantitated.

Inclusion-prone neuroblastoma cell experiments

Tet-inducible neuroblastoma cell line M17D-TR/αS-3K::YFP//RFP was generated by Lipofectamin 2000 (Invitrogen) co-transfecting pcDNA6/TR (Invitrogen) and described plasmid pcDNA4/αS-3K::YFP (Dettmer et al., 2015) followed by Blasticidin (1μg per mL) and Zeocin (200ng per mL) selection. Red fluorescent protein (RFP) expression was achieved by transduction with pLVX-IRES-mCherry (empty vector) viral particles. αS-3K::yellow fluorescent protein (YFP) expression was induced by adding 1ug per mL (f.c.) dox to culture media. Cultures then were treated with NOR at 0 (= DMSO alone at 0.1% f.c.), 0.3, 1, 3, 5 and 15μM. After treatments and dox induction, cells in culture dishes were incubated in the IncuCyte Zoom 2000 platform (Essen Biosciences) and images (red, green, bright field) were taken after 24 h. To measure inclusion formation in inducible M17D-TR/αS::YFP//RFP cells, we created the processing definition ‘Inclusions’. Inclusions (green objects) were defined using the following parameters in the IncuCyte Zoom 2016A software: Top-Hat background subtraction, radius 10μm, threshold (GCU) 5; Edge Split On, edge sensitivity 100; Cleanup, all parameters set to 0; Filters, Area (μm2): min 0 and max 100, Eccentricity: min 0.1, Mean Intensity: min 9.5, Integrated Intensity: min 200.0. Cells were plated in 384-well plates at 10,000 cells per well and induced 24 h after plating. Total Integrated RFP intensity was measured by the IncuCyte standard processing definition. After IncuCyte analysis, cell culture plates were stained with Hoechst dye (16.2μM f.c.) and fixed using 0.4% paraformaldehyde (f.c.) solution in PBS. YFP, RFP and Hoechst images were acquired on an IN-Cell 2200 platform. Ponceau staining and Western blotting of membranes using α-syn-specific antibodies C20 (Santa Cruz) and Syn-1 (BD Biosciences) have been described before (Dettmer et al., 2013).

Primary neuron culture experiments

Preparation of primary mesencephalic cultures—Primary midbrain cultures were prepared via dissection of E17 embryos obtained from pregnant Sprague-Dawley rats (Harlan, Indianapolis, IN) using methods approved by the Purdue Animal Care and Use Committee. The ventral mesencephalon containing the substantia nigra (SN) and ventral tegmental area (VTA) as isolated stereoscopically and dissociated with trypsin (final

concentration, 26 μg/ml in 0.9% [w/v] NaCl). The cells were plated at a density of 1250 cells per mm^2 on coverslips pre-treated with poly-L-lysine (5μg/ml) in media consisting of DMEM, 10% (v/v) FBS, 10% (v/v) horse serum, penicillin (100 U/ml), and streptomycin (100μg/ml). Four days later, the cells were treated with AraC (20μM, 48 h) to inhibit the growth of glial cells. After exposure to AraC, the cultures were incubated in fresh media for an additional 24 h. At this stage (i.e. 7 days *in vitro*), the neurons appeared differentiated with extended processes.

Lentiviral transductions and treatments with NOR—Lentivirus encoding the A53T α-syn variant was prepared using the ViraPower Lentivirus Expression System (Invitrogen). Primary cultures (7 days *in vitro*) were untreated or transduced with A53T lentivirus in media supplemented with polybrene (6μg/ml). Viral transductions were carried out at a multiplicity of infection (MOI, defined as the number of lentiviral particles per cell) of 10, in the absence or presence of NOR (0.3, 1.0, or 3μM). After 72 h, the cells were treated with fresh media (with or without NOR) for an additional 24 h prior to analysis.

Immunocytochemistry—The following antibodies were used: mouse anti-microtubule associated protein (MAP2; clone AP20, EMD Millipore/Chemicon), rabbit anti-tyrosine hydroxylase (TH; EMD Millipore/Chemicon), anti-mouse IgG-Alexa Fluor 488 (Invitrogen), and anti-rabbit IgG-Alexa Fluor 594 (Invitrogen). Primary midbrain cultures were fixed in 4% (w/v) paraformaldehyde in PBS for 30 min. The cells were permeabilized and blocked simultaneously for 1 h with PBS containing 1% (w/v) BSA, 10% (v/v) FBS, and 0.3% (v/v) Triton X-100. After washing with PBS, the cells were treated overnight at 4°C with antibodies specific for MAP2 (1:500) and anti-TH (1:500) in PBS with 1% (w/v) BSA. The cells were then washed with PBS and treated with secondary antibodies conjugated to Alexa Fluor 488 or Alexa Fluor 594 (both diluted at 1:1000 in PBS with 1% (w/v) BSA) for 1 h at 22°C. After a final wash with PBS, the coverslips were mounted onto slides using ProLong Gold Antifade reagent (Invitrogen), dried at room temperature overnight, and sealed with clear nail polish.

Measurement of primary neuron viability—Relative dopaminergic cell viability was assessed by counting MAP2- and TH-immunoreactive primary neurons in a blinded manner using a Nikon TE2000-U inverted fluorescence microscope with a 20X objective. Ten random fields of view were chosen for each sample to provide representation of the whole well. Approximately 150–350 $MAP2^+$ neurons were counted per experiment for each treatment. Replicate experiments were conducted using cultures isolated from 3 different pregnant rats. The data are expressed as the percentage of $MAP2^+$ neurons that were also TH^+ (this ratiometric approach was used to correct for variations in cell plating density). Primary neuron viability data were analyzed via repeated-measures, one-way ANOVA followed by Tukey's multiple comparisons *post hoc* test using GraphPad Prism 6.0 (La Jolla, CA). In analyzing percentage cell viability data by ANOVA, square root transformations were carried out to conform to ANOVA assumptions.

Transgenic *Drosophila* experiments

Transgenic Line—Transgenic *Drosophila* were created similar to Feany and Bender (2000). cDNA containing A30P mutant human α-syn (kind gift of M. Farrer, University of British Columbia and J. Hardy, University College London) was cloned downstream of the Glass Multimer Reporter promoter (Hay et al., 1997). Transgenic flies were created by germline transformation using the w^+ selectable marker. α-Syn expression was confirmed by Western blotting and immunohistochemistry. Retinal degeneration was measured by direct microscopic examination of the eye. In pseudopupil analysis, the intact eye is trans-illuminated and, in normal eyes, seven photoreceptors of each unit eye are arranged in a regular, trapezoidal pattern (ommatidia). The death of photoreceptor neurons leads to visible and quantifiable changes in these structures (Thomas and Wasserman, 1999). In the transgenic line used here, flies less than 24-hours-old have normal retinas as monitored by the pseudopupil assay. Retinas progressively degenerate over ten days until no normal ommatidia are visible, correlating with loss of photoreceptors and pigment cells. No degeneration is apparent in wild-type flies over that time.

Fly maintenance and NOR-embedded food—Flies were maintained on Formula 4–24 Instant *Drosophila* Medium from Carolina Biologicals (Burlington, NC) at 25°C with a constant light-cycle (12 hours light/dark). For treatment with NOR, Formula 4–24 was rehydrated with an aqueous solution of drug. Female flies (20 per vial) less than 12-hours-old were placed on mock treated or NOR-embedded food. Retinal degeneration was assessed on day 7 by pseudopupil analysis (Thomas and Wasserman, 1999). The analyzer was blinded to the identity of samples in all analyses. Fly heads were annealed to a glass microscope slide with clear nail polish. Eyes were trans-illuminated following optical neutralization of the corneas with immersion oil and examined under a 100X lens. An ommatidium was graded as normal if the normal complement of 7 intact rhabdomeres were visible, with all others classified as degenerate. 20–50 ommatidia were assessed per eye. The percent normal ommatidia was calculated for each eye and averaged for each group. Data was analyzed by one-way ANOVA followed by Dunnett's multiple comparison *post hoc* test using GraphPad Prism.

Transgenic mouse experiments

Transgenic line—Mice overexpressing human wild-type α-syn driven by the PDGF promoter (D-Line) were used (Masliah et al., 2000). Human α-syn over-expressing transgenic mice were raised in the QPS research animal facility under standardized conditions according to the animal welfare regulations of the Austrian guidelines for the care and use of laboratory animals and were approved by the Styrian government, Austria. Animals were provided with standard rodent chow (Altromin, Germany) and normal tap water *ad libitum*. Animals were housed under a constant light-cycle (12 hours light/dark). Genotyping of animals was done by tail tipping and were numbered consecutively by classical ear markings.

Experimental design—Six-month-old male transgenic mice were treated with vehicle (0.9% saline, n = 7) or 0.5 mg/kg (n=6), 5 mg/kg (n=6), or 25 mg/kg (n=7) NOR via once daily intraperitoneal (i.p.) injection for 30 days. Mice were euthanized by isoflurane

overdose and transcardially perfused with 0.9% saline. Brains were extracted and hemisected. The right hemisphere of all mice was immersion fixed in freshly produced 4% paraformaldehyde/PBS (pH 7.4) for one hour at room temperature. Thereafter brains were transferred to a 15% sucrose/PBS solution for 24 hours to ensure cryoprotection. On the next day brains were frozen in liquid isopentane and stored at −80°C until used. For quantitative immunohistochemistry, 10μm sections in the cortex and hippocampus were cryo-cut. Five sagittal sections from five different layers were used for counts of immunoreactive cells in the cortex and hippocampus. The 11th slice of each layer was taken for α-syn immunohistochemistry. Sections were stained with a NeuN antibody (1:800; Chemicon, MAB377) marked with a secondary Cy3 antibody (1:500; Jackson ImmunoResearch, 111-165-003) and with a human α-syn specific antibody (1:5; Alexis, 804-258-L001) marked with a secondary Cy2 antibody (Jackson ImmunoResearch, cat # 705-165-147). Fluorescence was recorded with an exposure time of 400ms and at 100X magnification. Quantitation of human α-syn immunoreactive cells was performed with Image Pro Plus (version 4.5.1.29). Up to 100 single images with 100-fold magnification each were assembled to one image (real size about 3 × 1 m), assuring a high pixel resolution for counting immunoreactive cells. Cell counts started with a detection step in which all assembled images were contrasted manually and the same intensity based threshold was used to mark all cells above the threshold intensity within the outlined brain region. A minimum size restriction of 30 μm^2 was set to exclude transversely cut neuritic processes and peripheral cell cuts from cells in consecutive slices. During this macro-based rating procedure the outlines of the object counts were saved. Next, all measured objects were extracted from the original (contrast free) image using the saved outlines and assembled according to object size in a sorted object image. The sorted object images were re-evaluated using a roundness restriction (Lower limit: 1 Upper limit: 1.5) to partition α-syn positive cells from bias objects. These automatic object counts were visually controlled and the count manually corrected by adding all explicit cells not being round enough or not separable from background, leading to the ultimate cell count. The measurement area of the cortex and the hippocampus in each slice and the relative and absolute number of α-syn immunoreactive cells per measurement area of the specific brain regions hippocampus and cortex were calculated. Data was analyzed by one-way ANOVA followed by Dunnett's multiple comparison *post hoc* test using GraphPad Prism.

Rat α-syn pre-formed fibril (PFF) model experiments

Animals—Adult male Sprague Dawley rats (200–225g; Harlan Laboratory, Indianapolis, IN) were utilized in all experiments. Studies were conducted at Michigan State University. Rats were housed in the Van Andel Research Institute vivarium. The animal facility is accredited by the Association for the Assessment and Accreditation of Laboratory Animal Care and complied with all Federal animal care and use guidelines. The Institutional Animal Care and Use Committee approved all protocols.

Intrastriatal α-syn pre-formed fibril (PFF) injections—Purification of recombinant, fulllength mouse α-syn protein and *in vitro* fibril assembly was performed as previously described (Luk et al., 2012). Immediately prior to injection, PFFs were thawed, diluted in sterile saline, and sonicated at room temperature using an ultrasonic homogenizer (300VT;

Biologics, Inc., Manassas, VA) with pulser at 20%, power output at 30% for 60 pulses at one second each. Anesthetized rats were placed into a stereotaxic device and PFFs were injected into the left striatum at one site (4μl/8μg protein; AP +1.6, ML +2.4, DV −4.2 from skull) at a rate of 0.5μl per minute. After each injection, the needle was left in place for 2 minutes and then slowly withdrawn. Animals were monitored weekly following surgery and euthanized at a time point when α-syn accumulation/aggregation is maximal (2 months post-injection) (Paumier et al., 2015a).

Experimental Design—*NOR Pre-treatment study.* Three-month-old male Sprague Dawley rats were randomized and divided into five treatment groups [saline (n=6), low dose NOR (5mg/kg; n=6); high dose NOR (15mg/kg; n=6)]. Daily intraperitoneal (i.p.) injections of saline or NOR commenced two weeks prior to PFF injection and continued for the duration of the study. Animals were euthanized 2 months post-PFF injection and processed for immunohistochemistry for morphological comparisons. *NOR Post-treatment study.* Three-month-old male Sprague Dawley rats were randomized and divided into three treatment groups [saline (n=10); low dose NOR (5mg/kg; n=10); high dose NOR (15mg/kg; n=10)]. All rats received an intrastriatal injection of sonicated pre-formed α-syn fibrils followed by daily i.p. injections of saline or NOR that began 2 weeks after PFF injection and continued for the duration of the study. Animals were euthanized 2 months post-injection and processed for immunohistochemistry for morphological comparisons.

Immunohistochemistry—Animals were euthanized via pentobarbital overdose (60mg/kg) and intracardially perfused with saline followed by cold 4% paraformaldehyde (PFA) in 0.1 M PO_4 buffer. Brains were removed and post-fixed in 4% PFA for 24 hours and sunk in 30% sucrose. Brains were frozen on a microtome platform and cut to generate 40μm thick sections. A 1:6 series of free-floating coronal sections was stained for either tyrosine hydroxylase (TH) or S129-phosphorylated α-syn (pSyn). Tissue was incubated in 0.3% H_20_2 for 45 minutes, rinsed and blocked in 10% normal goat serum (1 hour) then incubated in either primary mouse anti-pSyn (81a-1:15,000; Luk et al., 2012) or mouse-anti-TH (1:8000; Immunostar, Hudson, WI) antibodies overnight at 4°C. Then, sections were incubated in biotinylated secondary antisera against either mouse (1:400, Millipore, Temecula, CA) or rabbit IgG (1:400, Millipore, Temecula, CA) followed by Vector ABC detection kit (Vector Labs, Burlingame, CA). Antibody labeling was visualized by exposure to 0.5 mg/ml 3,3′ diaminobenzidine (DAB) and 0.03% H_2O_2 in Tris buffer. Sections were mounted on subbed slides, dehydrated to xylene and coverslipped with Cytoseal (Richard-Allan Scientific, Waltham, MA).

For all immunofluorescence a 1:12 series of free-floating coronal sections was stained. Tissue was rinsed and blocked in 10% new goat serum in TBS (1 hours) then incubated in primary solution 10% bovine serum albumin in TBS with appropriate primary antibody overnight at 4°C. Then, sections were incubated with corresponding Alexa Fluor antibodies in 10% new goat serum (1 hour). Double labeling was done simultaneously with primaries from two different host species followed by incubation with appropriate secondary antibodies. Primary antibodies used include rabbit anti-TH (1:4000; Millipore, Temecula, CA) and mouse anti-pSyn (81a-1:15,000). Secondary antibodies used include Alexa Fluor

568 goat anti-mouse IgG (1:500; Invitrogen, Carlsbad, CA) and Alexa Fluor 488 goat anti-rabbit IgG (1:500; Invitrogen, Carlsbad, CA).

pSyn aggregate counts—MicroBrightfield stereological software (MBF Bioscience, Williston, VT) was used to assess the total number of aggregates (defined as dense, darkly stained cores of phosphorylated α-syn staining) within the SN at the 60d time-point. A contour was drawn around the SN using a 4X objective and then aggregates were systematically counted using the 20X objective. The total number of aggregates was recorded for every sixth section throughout the rostro-caudal axis of the SN. The total number of aggregates for each section was compiled and reported as a total for each animal. Counts reflect actual numbers counted, not a population estimate derived from a sample within the SN.

Proteinase-K pretreatment—Confirmation of p-Syn positive inclusions as true aggregates was performed by exposing representative tissue sections to proteinase-K digestion prior to staining with the 81a antibody. Sections from four animals from each treatment group were randomly selected for exposure to proteinase-K. Sections were removed from cryoprotectant and washed 6-times for 10 min. each in 0.1M TBS pH 7.3. Sections were then treated with proteinase-K at a concentration of 10μg/ml in TBS for 10 minutes. Sections were washed 3-times for 10 min. each in 0.1M TBS. Finally, sections were stained for pSyn as detailed above.

Stereology—MicroBrightfield stereological software (MBF Bioscience, Williston, VT) was used to assess total population cell counts. Sections were counterstained with cresyl violet following TH immunolabeling in order to distinguish between loss of TH phenotype and neuronal loss. Glial nuclei were excluded from cresyl violet neuronal counts based on smaller size and homogeneous intense Nissl substance staining. Low magnification (1.25X) was used to outline the substantia nigra pars compacta (SNpc) and 20% of the designated area was sampled via a random series of counting frames (50μm × 50μm) systematically distributed across a grid (183μm × 112μm) placed over the SNpc. An investigator blinded to experimental conditions counted neurons using the optical fractionator probe (60X with oil). A marker was placed on each TH+ or cresyl-labeled neuron within the counting frame while focusing through a z-stack of images (1–2μm). Between 50 and 300 objects were counted to generate the stereological estimates. The total number of stained neurons was calculated using optical fractionator estimations and the variability within animals was assessed via the Gundersen Coefficient of Error (< 0.1).

α-Syn western blots—To determine whether NOR alters endogenous levels of α-syn in brain, an independent subset of rats were treated with either saline (n=3) or NOR (n=4; 15mg/kg) for 4 weeks. At the conclusion of the study, animals were euthanized and the striatum and midbrain regions were dissected on ice and processed for immunoblots. Tissue samples were homogenized in lysis buffer (T-PER) and protein determination was performed (Pierce). Lysates (20μg) were separated on 4–12% Bis-Tris gels (Invitrogen; Carlsbad, CA) and then transferred onto nitrocellulose membranes (Invitrogen, Carlsbad, CA). The blots were probed with the following antibodies: rabbit polyclonal α-syn (1:2,000;

Santa Cruz, Dallas, TX), mouse monoclonal actin (1:10,000, Sigma, Saint Louis, MO), followed by goat anti-rabbit (1:10,000; Novus, Littleton, CO) and goat-anti-mouse (1:10,000; Novus, Littleton, CO). Protein bands were detected and quantified with the OdysseyClx infrared scanning system (LiCor, Lincoln, Nebraska).

Retrograde transport of fluorogold—To ensure the reduction in aggregation was not due to blockade of retrograde transport an additional cohort of rats were treated with either saline (n=3), or NOR (n=4 at 5mg/kg; n=4 at 15mg/kg) for 2 weeks prior to an intrastriatal injection of fluorogold (1 injection site AP +1.6 ML +2.4 DV −4.2 from skull, 2μl volume, rate 0.5μl/min., 4% solution fluorogold (Fluorochrome LLC, Denver, CO)). Brains were processed three days post-injection and immunofluorescence was examined to assess magnitude of fluorogold transport across groups.

Statistical analysis—All statistical tests were completed using GraphPad Prism software (version 6, GraphPad, La Jolla, CA). Differences between three or more groups were analyzed using a one-way ANOVA. Post-hoc comparisons were made between groups using either Dunnett's multiple comparisons or Bonferroni's correction method. The level of significance was set at $P<0.05$.

α-Syn molecular reconfiguration experiments

α-Synuclein Mutation, Expression and Purification—The α-syn plasmid was a kind gift from Gary Pielak (University of North Carolina, Chapel Hill, NC). The α-syn mutant containing the tryptophan/cysteine (Trp/Cys) pair A69C/F94W was created using the QuikChange site-directed mutagenesis kit (Stratagene). The mutants was then expressed in E. coli BL21 (DE3) cells and purified by a procedure described previously (Ahmad et al. 2012). The monomeric α-syn peak obtained using size exclusion was found to be >95% pure as assessed by SDS-PAGE and Coomassie blue staining. The protein was stored at −20°C in aliquots of 300μM.

NOR binding studies—All fluorescence measurements were conducted in PTI Q4 fluorimeter equipped with a temperature controlled cuvette holder and stirrer kit. Fluorescence of W94 was measured at room temperature in a 1cm path length cuvette. The excitation wavelength was 280nm. The protein concentration was kept fixed at 3μM and the NOR concentration was added to the protein with increasing concentrations, ranging from 2nM to 30μM. All spectra at all concentrations were analyzed globally using single value decomposition (svd).

Trp-Cys contact quenching measurements—Monomeric α-syn was mutated to contain one Trp and one Cys (A69C/Y94W). The tryptophan is excited to a long-lived excited state that is quenched on contact with cysteine. The measurement of the tryptophan triplet state lifetime has been described in detail previously. Briefly, the triplet state was excited by a 10ns laser pulse at 289nm created by the 4^{th}-harmonic of a Nd:YAG laser (Continuum, Surelite II) and a 1-meter Raman Cell filled with D_2 gas. The population of the triplet state was probed by continuous absorption of a diode laser at 450nm (91Laser LSR445NL) and probe and reference beams are detected by silicon optical detectors

(Newport 2151). These signals are combined in a differential amplifier (DA 1853A, LeCroy) and further amplified in a 350 MHZ preamplifier (SR445A, Stanford Research Systems) for a total gain of 50X. The temperature in the instrument is set by a thermoelectric-controlled cuvette holder (Quantum Northwest FLASH 100). All measurements were completed within 30 minutes, much less than the observed lag times for α-syn aggregation under these conditions (~60 hrs). For each measurement, an aliquot of the protein was thawed and diluted 10x in 25mM sodium phosphate buffer (pH=7.5), 10mM TCEP (to prevent disulfide bond formation) and various sucrose concentrations (0, 10, 20 and 30% w/w). The buffer, sucrose and TCEP solutions were bubbled with N_2O for one hour to eliminate oxygen and scavenge solvated electrons created in the UV laser pulse. The viscosity of each sucrose concentration at different temperatures was measured independently using a cone-cup viscometer (Brookfield Engineering). Each sucrose concentration was measured at five temperatures (0, 10, 20, 30 and 40°C).

To measure intramolecular diffusion, we excite W94 to a long-lived triplet state which is quenched upon close contact with C69, almost 400-times more efficiently than with any other amino acid. The theory of Szabo, Schulten and Schulten (1980) gives reaction-limited and diffusion-limited rates as

$$k_R = \int_{d_\alpha}^{l_c} q(r)P(r)dr$$

$$\frac{1}{k_{D+}} = \frac{1}{k_R^2 D}\int_{d_\alpha}^{l_c} \frac{dr}{P(r)}\left\{\int_r^{l_c}\left(q(x)-k_R\right)P(x)dx\right\}^2$$

where the integration limits are d_α =4 Å, and l_c, the contour length of the protein. P(r) is the probability of intrachain distances, r is the distance between the Trp and Cys, and $q(r) = 4.2x10^9 \exp(-4.0(r-4.0))\ s^{-1}$ is the experimentally-determined distance-dependent quenching rate. This rate for the Trp-Cys system drops off very rapidly beyond 4.0 Å, so the reaction-limited rate is mostly determined by the probability of the shortest distances (Lapidus et al., 2001).

$$P(r) = \frac{4\pi r^2}{N}\left(\frac{3}{2\pi\langle r^2\rangle}\right)^{3/2}\exp\left(-\frac{3r^2}{2\langle r^2\rangle}\right)$$

To determine D we assume the probability distribution, $P(r)$, for each mutant and temperature is given by a Gaussian chain model where $\langle r^2\rangle$, the average Trp-Cys distance, is an adjustable parameter, and N is a normalization constant such that $\int P(r) = 1$. For each mutant and temperature, $\langle r^2\rangle$ was found such that the calculated k_R from the equation in text Figure 8 matched the measured rate. These values are almost certainly too big because the real distribution is narrower than a Gaussian so that we must choose a large $\langle r^2\rangle$ in order to make the probability low enough at the shortest distances. However for purposes of comparison with and without NOR, it is a suitable approximation. Finally, the diffusion

coefficient, *D,* is computed from the equation above with the appropriate *P(r)* and the measured k_{D+}.

Results

NOR delays aggregation of α-syn *in vitro*

To test whether NOR can affect α-syn aggregation *in vitro*, recombinant wild-type α-syn monomer was incubated with NOR or vehicle with gentle agitation at 37°C. Aggregation progression was monitored by fluorescence polarization (FP) using an Alexa-Fluor-594 α-syn adduct as a tracer (Luk et al., 2007). NOR increased the lag time to initiation of aggregation in a dose-dependent fashion (Figure 1A). To determine if the delay in aggregation is related to conversion of monomer to higher molecular weight conformations, the reaction product was separated by size exclusion. In this assay, loss of monomer was detected in parallel with the formation of species associated with high FP. Addition of NOR to the reaction delayed the loss of monomer (Figure 1B&C). This is consistent with NOR delaying initiation of aggregation through interaction with monomeric α-syn and inhibiting formation of high molecular weight species.

NOR reduces aggregation and neurotoxicity of α-syn in cell and animal models

NOR inhibits accumulation of α-syn inclusions in cultured inclusion-prone neuroblastoma cells—α-Syn E35K+E46K+E61K (= αS3K) is an ‘amplification’ of the familial PD-linked α-syn mutation E46K and readily forms round cytoplasmic inclusions in cultured cells (Dettmer et al., 2015). A stable neuroblastoma cell line was generated that expresses an α-syn-3K::yellow fluorescent protein (YFP) fusion protein (dox-inducible) and red fluorescent protein (RFP; constitutive). Twenty-four hour dox-induction of α-syn-3K::YFP led to pronounced round inclusions in the presence of vehicle alone, whereas NOR dose-dependently prevented their occurence (Figure 2a and 2c, top row). RFP intensity (Figure 2b and 2c, middle row) and nuclei count (Figure 2c, bottom row) were not affected, ruling out cell loss as the mechanism of decreased detection of aggregates in NOR-treated cultures. Western blotting for α-syn using two different antibodies showed that levels were unaffected by the treatments (Figure 2d, panels on the left) and Ponceau staining of the same membranes (Figure 2d, panels on the right) confirmed equal loading and equivalent protein content in all treated cells.

NOR suppresses neurotoxicity in cultured dopamine neurons expressing A53T α-syn—Transduction of embryonic rat midbrain cultures with a lentivirus encoding mutant A53T α-syn is associated with development of insoluble (SDS-resistant) α-syn conformations and selective degeneration dopamine (DA) neurons (Cooper et al., 2006; Liu et al., 2008). Prior to examining the effects of NOR on A53T α-syn transduced cultures, we performed a pilot experiment to determine whether NOR affected lentivirus transduction of LacZ-V5 in cultured midbrain neurons. Western blot analysis revealed no effect of NOR on transduction. Expression of A53T α-syn in midbrain cultures resulted in a significant decrease in survival of TH-positive neurons. Treatment with 1μM and 3μM NOR significantly increased the survival of DA neurons (Figure 3A).

NOR rescues α-syn neurotoxicity in transgenic Drosophila—Death of photoreceptor neurons in *Drosophila* has been used as a model of neurodegeneration induced by toxic proteins such as α-syn and mutant huntingtin (Feany and Bender, 2000; Steffan et al., 2001; Ehrnhoefer et al., 2006). NOR was tested in A30P α-syn transgenic *Drosophila* that exhibit progressive retinal degeneration following over-expression specific to the eye (GMR-GAL4/+). Flies less than 24-hours old have normal retinas, but exhibit complete degeneration of ommatidia by day 10 post-hatching. Within 12 hours of hatching, α-syn transgenic flies were transferred to food supplemented with NOR or vehicle, and evaluated for retinal degeneration after seven days. Transgenic flies that ingested NOR-embedded food had significantly more normal ommatidia than those raised on untreated food. Suppression of α-syn-induced retinal degeneration was dose dependent (Figure 3B).

NOR reduces accumulation of α-syn in transgenic mice—The Line-D transgenic mouse model exhibits progressive accumulation of human α-syn, driven by the platelet-derived growth factor (PDGF) promoter, between 3 and 12 months of age (Masliah et al., 2000; Amschl et al., 2013). In these animals, human α-syn accumulates in synapses of the neocortex, limbic system and olfactory regions and form inclusion bodies in neurons of the deep layers of neocortex and pyramidal cells of the hippocampus (Rockenstein et al., 2002). At an early stage of development of α-syn pathology in these animals, six-month-old transgenic mice were administered NOR or vehicle by intraperitoneal injection once daily for one month. Human α-syn in the cortex and hippocampus was analyzed by immunohistochemistry. NOR inhibited the progression of α-syn pathology in a dose-related pattern compared to vehicle treated animals in both brain regions (Figure 4).

NOR attenuates development of α-syn aggregates in the rat pre-formed fibril (PFF) injection model—The recently established rat synucleinopathy model is based on direct brain injection of a fibrillar form (pre-formed fibrils; PFF) of α-syn that seeds endogenous α-syn, that progressively accumulates, aggregates and leads to degeneration of substantia nigra (SN) DA neurons over a 6 month time course (Paumier et al., 2015). Prior to neurodegeneration, at two months following injection of α-syn PFFs into the striatum of young adult rats, TH-positive neurons of the SN display numerous intracellular α-syn inclusions that stain positive for phosphorylation at Ser 129 (pSyn) (Fujiwara et al., 2002) (Figure 5A&C) and are proteinase-K resistant (Figure 5C′), supporting their identity as insoluble α-syn aggregates. When rats received once daily intraperitoneal injection of NOR in a pretreatment paradigm, beginning 2 weeks prior to PFF injection and continuing for the remaining 8 weeks of the study, NOR significantly reduced the accumulation of aggregates in SN in a dose related manner (Figure 5B,D, E, F).

The effect of NOR treatment also was assessed in a post-PFF infusion design to determine whether NOR had an impact on clearance of pre-existing aggregates. α-Syn PFFs were injected into the striatum, and 2 weeks later subjects were randomly assigned to groups that received daily saline or NOR injection, for an additional 6 weeks. Over this interval, saline treated animals showed the expected continued accumulation of aggregates in SN. NOR treated animals exhibited a consistent, modest reduction in accumulation of aggregates: 5mg/kg = −30%, 15mg/kg = −29%. These differences did not reach statistical significance.

Taken together, the findings suggest that NOR has the capacity to delay and diminish formation of α-syn aggregates, but once seeding and aggregation is established, NOR does not clear existing pathology.

In the rat PFF synucleinopathy model, reduced numbers of aggregates is not attributable to NOR-induced cell death, reduced levels of endogenous α-syn or impaired retrograde transport—We examined several possible caveats to the reduced presence of pSyn aggregates in NOR treated PFF injected rats, including NOR toxicity producing loss of neurons, reduction of endogenous α-syn available for templating and aggregation, and impaired retrograde axonal transport of PFF-templated seeds. We previously demonstrated that at the 8 week post-PFF time point examined here, overt loss of DA neurons has yet to occur (Paumier et al., 2015). Stereological counts of TH-positive neurons and cresyl violet stained neurons in SN were not changed with NOR treatment (Figure 6A&B), consistent with the absence of a toxic effect. Western blot analysis of endogenous α-syn levels in untreated rats and those treated with NOR for 30 days did not differ (Figure 6C), consistent with no association of NOR treatment with reduced endogenous α-syn available for templating by PFFs. Injection of the retrograde tracer fluorogold into the striatum of untreated rats and those treated with NOR revealed no impairment of axonal transport as a contributor to reduced aggregate formation (Figure 6D).

A mechanism for NOR inhibition of α-syn aggregation

We conducted a series of experiments to test a potential mechanism of action of reduced aggregation of α-syn with exposure to NOR based on the hypothesis that aggregation is kinetically controlled by reconfiguration of α-syn monomers (Lapidus, 2013). This hypothesis contends that when two monomers come into contact, stabilizing interactions must be made within the time of the encounter complex in order to form an oligomer. The opportunity for stabilizing interactions to occur is regulated by the rate at which the unstructured monomer ensemble changes its conformation: faster internal reconfiguration reduces the opportunity for bimolecular stabilization leading to aggregation.

Intramolecular diffusion of α-syn can be assessed by measurement of intramolecular contact between two probes placed into the amino acid chain (Ahmad et al., 2012). Ideally, these measurements require a long-lived probe that is quenched on contact with an efficient quencher located in the same chain. For our analysis this is accomplished using the triplet state of tryptophan (Trp) as the probe and cysteine (Cys) to efficiently quench the triplet state only upon close contact (Trp-Cys quenching). An α-syn mutant was engineered that contains exactly one tryptophan and one cysteine in the sequence (A69C/Y94W). This mutation does not alter aggregation kinetics (Ahmad et al., 2012), and as a side benefit, allows detection of conformational changes by tryptophan fluorescence. Empirically, we have observed that an increase in reconfiguration is correlated with more expanded and solvent-exposed conformations (Ahmad et al. 2012).

Figure 7a shows the emission spectra of W94 with varying concentrations of NOR. There is a significant red shift, even with addition of nanomolar (nM) concentrations of NOR, indicating higher solvent exposure of W94 consistent with a more expanded conformation of

the α-syn chain. In addition, we examined the response to Sypro Orange, a fluorophore that increases emission when bound to hydrophobic residues. Figure 7b shows the emission of Sypro Orange when bound to α-syn and with the addition of NOR. The increase in fluorescence with the addition of NOR indicates more hydrophobic residues within the chain are exposed to solvent and available to bind Sypro Orange. Overall these fluorescence signals suggest that α-syn becomes more expanded and more solvent exposed upon binding with NOR.

The general scheme of the Trp-Cys quenching experiment is shown in Figure 8a. Pulsed optical excitation leads to population of the lowest excited triplet state of Trp. Trp contacts Cys in a diffusion-limited process, and then either diffuses away or is quenched by Cys. The observed rate of Trp triplet decay is given by

$$k_{obs}=\frac{k_{D+}q}{k_{D-}+q} \quad (1)$$

and can be decomposed into two rates, a reaction-limited rate (k_R), which depends on temperature, and a diffusion-limited rate (k_{D+}), which depends on both temperature and viscosity.

$$\frac{1}{k_{obs}}=\frac{1}{k_{D+}}+\frac{1}{qK}=\frac{1}{k_{D+}(T,\eta)}+\frac{1}{k_R(T)} \quad (2)$$

By measuring the Trp triplet decay rate at various viscosities at a particular temperature, we can extract these rates from a plot of triplet lifetimes vs. viscosity. The intercept of a linear fit of this data is $1/k_R$ and the slope is $1/k_{D+}$, normalized by the viscosity of water at that particular temperature. The reaction-limited and diffusion-limited rates at 30°C are plotted for α-syn protein alone and the protein with 1:1 NOR (Figure 8b). With addition of NOR, the reaction-limited rate decreases and the diffusion-limited rate increases.

To interpret the reaction-limited and diffusion-limited rates we use a theory by Szabo, Schulten and Schulten (1980), which models protein dynamics as diffusion on a 1-d potential determined by the probability of Trp-Cys distances. The reaction-limited rate is inversely proportional to the volume of the chain. Thus, the decrease in k_R with the addition of NOR indicates the chain is more expanded. The diffusion-limited rate is inversely proportional to the volume of the chain and directly proportional to the intramolecular diffusion coefficient, D. The moderate increase in k_{D+} with the addition of NOR reflects both the expansion of the chain (which would decrease the rate) and a larger increase in the rate of intramolecular diffusion (reconfiguration of the α-syn chain) D (Figure 8c).

As stated above, the first step of aggregation is controlled by the rate of monomer reconfiguration, defined as $k_f=D/RG^2$, where D is the intramolecular diffusion coefficient and R_G is the radius of gyration. While D increases by ~10x with NOR, any changes in R_G

are more modest, on the order of 10% (Ahmad et al., 2012). Therefore, changes in reconfiguration rate are essentially changes in intramolecular diffusion. In the absence of NOR, it is possible for α-syn to form oligomers because the reconfiguration rate is similar to the bimolecular rate. However, with the addition of NOR, the reconfiguration rate increases significantly and is much faster than the bimolecular rate. Thus, during the encounter complex with another monomer, each monomer can reconfigure to escape stabilizing interactions and oligomer (O) formation leading to aggregation. This hypothesis can be summarized with the following kinetic model (Lapidus, 2013):

$$\begin{array}{c} M \underset{k_{-1}}{\overset{k_1}{\rightleftarrows}} M* \\ M*+M* \xrightarrow{k_{bi}} [M*M*] \xrightarrow{k_O} O \\ \downarrow k_{-1} \\ M+M* \end{array} \quad \text{(i)}$$

Solutions to scheme (i) are shown in Figure 8d for $k_r=k_1+k_{-1} = D/RG^2$. We assume $K=k_{-1}/k_1 = 1$ for simplicity and k_o=100 s^{-1} for computational ease. The Fick model of diffusion gives $k_{bi} = 4\pi\iota(D_M + D_{M^*})N_A/1000 = 3.8\times10^8$ $M^{-1}s^{-1}$. In aggregation experiments in this work (Figure 1), the concentration was 70μM, therefore k_{bi}=26,600 s^{-1}. Using the values for D given in Figure 8c and R_G = 30 Å, a reasonable assumption for the size of α-syn, we can solve the model in scheme (i) and plot the concentration of oligomers formed [O]. A fit of each curve in Figure 8d to a second-order formation function, yields a formation rate of 5.0 s^{-1} without NOR and 0.65 s^{-1} with NOR, an almost 8-fold decrease in oligomerization rate.

Further steps to convert the oligomer to fibrils would not be sensitive to the reconfiguration rate but also could be altered by the binding of NOR. In the α-syn PFF model, it has been demonstrated that α-syn spread and aggregation is via secondary nucleation (Volpicelli-Daley et al., 2011). If the nucleating species is the encounter complex, [M*M*], then keeping this complex short-lived by increasing the reconfiguration rate with NOR would impede this process. Thus, the conclusion drawn from the *in vitro* experiments is that upon binding of NOR, the intrinsically disordered α-syn becomes more solvent exposed, more diffusive and resistant to fibrilization.

Discussion

NOR is a second-generation tricyclic antidepressant (TCA) medication with a long history of safety and efficacy in the treatment of depression and chronic pain. Evidence from multiple studies assessing the mechanisms of action of TCAs in model systems with no direct relevance to PD indicate that this class of compounds have multiple properties that suggest the potential for neuroprotection, including, increased expression of factors associated with neural plasticity (Nibuya et al., 1996; Sairanen et al., 2007; Boehm et al., 2006), stimulation of neurotrophic factor signaling (e.g., brain-derived neurotrophic factor (BDNF) (Nibuya et al., 1995; Xu et al., 2003; Balu et al., 2008), direct binding to neurotrophic factor receptors (TrkA&B)(Cong et al., 2015; Jang et al., 2009; Rantamäki et al., 2011), activation of autophagy (Zschocke and Rein, 2011; Gassen et al., 2014), reduced

neuroinflammation (Kubera et al., 2000; Obuchowicz et al., 2006; Sadeghi et al., 2011; Valera et al., 2014), and stimulation of neurogenesis (Chadwick et al., 2011; Boldrini et al., 2009; Boku et al., 2013). Coinciding with increased awareness of the high prevalence of depression in PD (Dooneief et al., 1992; McDonald et al., 2003), we became interested in whether the neuroprotective properties of TCAs might impact nigrostriatal system degeneration in PD models. In addition, our attention was drawn to TCAs as they have proven to be superior in treating depression associated with PD (Frisina et al., 2008; Menza et al., 2009). Work in one of our laboratories demonstrated that the TCA amitriptyline (AMI) reduced nigrostriatal degeneration in a rat 6-hydroxydopamine toxin model of PD and was associated with increased levels of BDNF in basal ganglia structures (Paumier et al., 2015b). Also, we conducted a retrospective data analysis of clinical trials involving newly diagnosed PD patients that specifically identified TCAs as the only class of antidepressant medications associated with a significant delay in need for dopaminergic therapy (Paumier et al., 2012).

In the present series of experiments, we utilized the TCA compound NOR as representative of this class of drugs. NOR is the major metabolite of AMI, and NOR accumulates in brain following chronic administration of AMI (Coudore et al., 1996). Here, we present evidence that NOR protects against the negative consequences of pathological α-syn in cell culture models, transgenic flies and mice, and injection of α-syn PFFs in rats. The cell and animal models in our studies include multiple mutant forms of α-syn in addition to wildtype α-syn, vary in their cellular and regional accumulation of α-syn, whether aggregates form, and whether the result is neurotoxicity. However, all of the model systems provide direct links to α-syn pathology that is diminished by treatment with NOR. Indeed, the inhibitory effects of NOR in all of these models argues for the broad applicability of NOR as an α-syn anti-aggregation compound.

Arguably, the rat PFF model most closely resembles events associated with α-syn pathology in PD, incorporating seeding, accumulation and development of aggregates within midbrain DA neurons, ultimately leading to neurodegeneration (Paumier et al., 2015a). The significant dose-related decrease in α-syn aggregates with NOR pre-treatment, and partial effects with NOR post-treatment, suggest that while NOR does not appear to clear existing pathology, it interrupts the ongoing processes related to formation and accumulation of neurotoxic α-syn conformations. This suggests a direct interaction of NOR with non-fibrillar α-syn and we hypothesize that NOR interacts directly with the monomer and prevents the earliest stages of aggregation.

We tested this hypothesis using multiple *in vitro* aggregation and kinetics assays that suggest NOR directly binds to the monomeric form of α-syn and inhibits aggregation. We used the method of Trp-Cys quenching to measure intramolecular diffusion: the random motion of one part of the protein chain relative to another. Using this assay, Lapidus and collaborators have demonstrated that their findings are consistent with a model of α-syn aggregation in which intramolecular reconfiguration of the monomer determines the rate of bimolecular association and subsequent steps in aggregation (Ahmad et al., 2012). They have gone on to demonstrate that PD-causing mutations of α-syn slow down intramolecular diffusion of the protein chain, predicting the propensity for aggregation (Acharya et al., 2015). They posit

that one therapeutic strategy for PD and other synucleinopathies is to use small molecules that bind to α-syn and increase its reconfiguration rate under physiological conditions, thereby preventing aggregation. Consistent with this view, they have shown that both the synthetic molecular tweezer CLR01 and the natural substance curcumin bind to monomeric α-syn, increase its reconfiguration rate and inhibit aggregation (Acharya et al., 2014; Basir and Lapidus, 2012). The results reported here indicate that NOR exhibits the most potent effects to date, binding to monomeric α-syn at nM concentrations and reducing oligomerization nearly 8-fold. Intrinsically disordered proteins are now recognized as drug targets (Metallo, 2010). In fact, a recent effort to discover small molecule α-syn aggregation inhibitors specifically targeted the monomer ensemble (Tóth et al., 2014). However, characterizing such protein-ligand interactions is challenging due to the lack of globular structure, existence of many possible transient binding sites, and probability that a ligand may bind to only a subset of disordered states (Tóth et al., 2014; Zhu et al., 2013). Our approach was to examine how a ligand might change the ensemble of disordered structures and the dynamics of reconfiguration of that ensemble.

In addition to avoiding formation of potentially toxic oligomers, an intriguing potential benefit of preventing monomer aggregation is preserving the normal functions of α-syn. While aggregation of α-syn in synucleinopathies is commonly interpreted as gain-of-function toxicity the converse may be true: sequestration of native forms of α-syn in aggregates may decrease the functional pool, resulting in loss-of-function toxicity (Perez and Hastings, 2004; Cookson, 2006; Kanaan and Manfredsson, 2012; Collier et al., 2016). For example, SNARE-chaperone activity requires a balance between soluble monomer and membrane-bound helical conformers (Burré et al., 2015). By diminishing misfolding, NOR could normalize the concentration of available monomer for membrane binding in neurons and preserve normal function.

Although several small molecule fibrillization inhibitors have been identified, none have yet proven therapeutically useful for synucleinopathies in the clinic. The properties of NOR suggest that specific interaction with the unstructured form of α-syn may be critical for novel therapeutics. However, it remains to be determined whether specific targeting of α-syn represents an optimal approach to treatment for synucleinopathies, or whether complex disorders require a multi-target approach best served by combination therapies (Valera and Masliah, 2016). The present findings indicate that NOR, a tricyclic antidepressant with a long history of safety and efficacy, may provide multiple benefits for these syndromes, including amelioration of comorbid depression, modulation of important signaling pathways involved in cell survival and plasticity, reduced inflammation and interference with misfolding and aggregation of α-syn : a multifunction compound to treat a complex disorder.

Acknowledgments

We thank Kelvin Luk for the generous gift of mouse α-syn preformed fibrils (PFF) used in the rat PFF model, Gary Pielak for the kind gift of α-syn plasmid used in anti-aggregation assays, and Matt Farrer and John Hardy for the kind gift of cDNA containing the A30P human α-syn mutation used in the creation of transgenic Drosophila. We are grateful for the excellent technical assistance of Stephanie Celano, Emily Schulz, Alix Booms and Brian Daley. This work was supported by funds provided by the Saint Mary's Foundation (KLP), Michael J Fox Foundation (KLP, TJC) and NIH awards NS058830, NS094460 (TJC) and GM100908 (LJL).

References

Abeliovich A, Schmitz Y, Fariñas I, Choi-Lundberg D, Ho WH, Castillo PE, Shinsky N, Verdugo JM, Armanini M, Hynes RA, Phillips H, Sulzer D, Rosenthal A. Mice lacking alpha-synuclein display functional deficits in the nigrostriatal dopamine system. Neuron. 2000; 25:239–252. [PubMed: 10707987]

Acharya S, Safaie BM, Wongkongkathep P, Ivanonva MI, Attar A, Klärner F-G, Schrader T, Loo JA, Bitan G, Lapidus LJ. Molecular basis for preventing α-synuclein aggregation by a molecular tweezer. J Biol Chem. 2014; 289:10727–10737. [PubMed: 24567327]

Acharya S, Saha S, Ahmad B, Lapidus LJ. Effects of mutations on the reconfiguration rate of α-synuclein. J Phys Chem B. 2015; 119:15443–15450. [PubMed: 26572968]

Ahmad B, Chen Y, Lapidus LJ. Aggregation of α-synuclein is kinetically controlled by intramolecular diffusion. Proc Natl Acad Sci USA. 2012; 109:2336–2341. [PubMed: 22308332]

Ahmad B, Lapidus LJ. Curcumin prevents aggregation in α-synuclein by increasing reconfiguration rate. J Biol Chem. 2012; 287:9193–9199. [PubMed: 22267729]

Amschl D, Neddens J, Havas D, Flunkert S, Rabl R, Römer H, Rockenstein E, Masliah E, Windisch M, Hutter-Paier B. Time course and progression of wild type α-synuclein accumulation in a transgenic mouse model. BMC Neurosci. 2013; 14:6. [PubMed: 23302418]

Balu DT, Hoshaw BA, Malberg JE, Rosenzweig-Lipson S, Schechter LE, Lucki I. Differential regulation of central BDNF protein levels by antidepressant and non-antidepressant drug treatments. Brain Res. 2008; 1211:37–43. [PubMed: 18433734]

Boehm C, Newrzella D, Herberger S, Schramm N, Eisenhardt G, Schenk V, Sonntag-Buck V, Sorgenfrei O. Effects of antidepressant treatment on gene expression profile in mouse brain: cell type-specific transcription profiling using laser microdissection and microarray analysis. J Neurochem. 2006; 97(Suppl 1):44–49.

Boku S, Hisaoka-Nakashima K, Nakagawa S, Kato A, Kajitani N, Inoue T, Kusumi I, Takebayashi M. Tricyclic antidepressant amitriptyline indirectly increases the proliferation of adult dentate gyrus-derived neural precursors: an involvement of astrocytes. PLoS One. 2013; 8:e79371. [PubMed: 24260208]

Boldrini M, Underwood MD, Hen R, Rosoklija GB, Dwork AJ, John Mann J, Arango V. Antidepressants increase neural progenitor cells in the human hippocampus. Neuropsychopharmacol. 2009; 34:2376–2389.

Burré J, Sharma M, Sudhöf TC. Definition of a molecular pathway mediating α-synuclein neurotoxicity. J Neurosci. 2015; 35:5221–5232. [PubMed: 25834048]

Burré J, Sharma M, Südhof TC. α-Synuclein assembles into higher-order multimers upon membrane binding to promote SNARE complex formation. Proc Natl Acad Sci USA. 2014; 111:E4274–4283. [PubMed: 25246573]

Burré J, Sharma M, Tsetsenis T, Buchman V, Etherton MR, Sudhöf TC. Alpha-synuclein promotes SNARE-complex assembly in vivo and in vitro. Science. 2010; 329:1663–1667. [PubMed: 20798282]

Chadwick W, Mitchell N, Caroll J, Zhou Y, Park SS, Wang L, Becker KG, Zhang Y, Lehmann E, Wood WH 3rd, Martin B, Maudsley S. Amitriptyline-mediated cognitive enhancement in aged 3xTg Alzheimer's disease mice is associated with neurogenesis and neurtrophic activity. PLoS One. 2011; 6:e21660. [PubMed: 21738757]

Chiti F, Dobson CM. Protein misfolding, functional amyloid, and human disease. Annu Rev Biochem. 2006; 75:333–366. [PubMed: 16756495]

Collier TJ, Redmond DE Jr, Steece-Collier K, Lipton JW, Manfredsson FP. Is alpha-synuclein loss-of-function a contributor to parkinsonian pathology? Evidence from non-human primates. Front Neurosci. 2016; 10:12. [PubMed: 26858591]

Cong WN, Chadwick W, Wang R, Daimon CM, Cai H, Amma J, Wood WH 3rd, Becker KG, Martin B, Maudsley S. Amitriptyline improves motor function via enhanced neurotrophin signaling and mitochondrial functions in the murine N171-82Q Huntington disease model. J Biol Chem. 2015; 290:2728–2743. [PubMed: 25505248]

Conway KA, Harper JD, Lansbury PT. Accelerated in vitro fibril formation by a mutant alpha-synuclein linked to early-onset Parkinson disease. Nat Med. 1998; 4:1318–1320. [PubMed: 9809558]

Cookson MR. Hero versus anti-hero: the multiple roles of alpha-synuclein in neurodegeneration. Exp Neurol. 2006; 199:238–242. [PubMed: 16687141]

Cooper AA, Gitler AD, Cashikar A, Haynes CM, Hill KJ, Bhullar B, Liu K, Xu K, Strathearn KE, Liu F, Cao S, Caldwell KA, Caldwell GA, Marsischky G, Kolodner RD, Labaer J, Rochet JC, Bonini NM, Lindquist S. Alpha-synuclein blocks ER-Golgi traffic and Rab1 rescues neuron loss in Parkinson's models. Science. 2006; 313:324–328. [PubMed: 16794039]

Coudore F, Besson A, Eschalier A, Lavarenne J, Fialip J. Plasma and brain pharmacokinetics of amitriptyline and its demethylated and hydroxylated metabolites after one and six half-life repeated administrations to rats. Gen Pharmac. 1996; 27:215–219.

Dettmer U, Newman AJ, Luth ES, Bartels T, Selkoe D. In vivo cross-linking reveals principally oligomeric forms of α-synuclein and β-synuclein in neurons and non-neural cells. J Biol Chem. 2013; 288:6371–6385. [PubMed: 23319586]

Dettmer U, Newman AJ, Soldner F, Luth ES, Kim NC, von Saucken VE, Sanderson JB, Jaenisch R, Bartels T, Selkoe D. Parkinson-causing α-syn missense mutations shift native tetramers to monomers as a mechanism for disease initiation. Nature Comm. 2015; 6:7314.

Dooneief G, Mirabello E, Bell K, Marder K, Stern Y, Mayeux R. An estimate of the incidence of depression in idiopathic Parkinson's disease. Arch Neurol. 1992; 49:305–307. [PubMed: 1536634]

Ehrnhoefer DE, Duennwald M, Markovic P, Wacker JL, Engemann S, Roark M, Legleiter J, Marsh JL, Thompson LM, Lindquist S, Muchowski PJ, Wanker EE. Green tea (−)-epigallocatechin-gallate modulates early events in huntingtin misfolding and reduces toxicity in Huntington's disease models. Hum Mol Genet. 2006; 15:2743–2751. [PubMed: 16893904]

Feany MB, Bender WW. A Drosophila model of Parkinson's disease. Nature. 2000; 404:394–398. [PubMed: 10746727]

Frisina PG, Tenenbaum HR, Borod JC, Foldi NS. The effects of antidepressants in Parkinson's disease: a meta-analysis. Int J Neurosci. 2008; 118:667–682. [PubMed: 18446583]

Fujiwara H, Hasegawa M, Dohmae N, Kawashima A, Masliah E, Goldberg MS, Shen J, Takio K, Iwatsubo T. α-Synuclein is phosphorylated in synucleinopathy lesions. Nature Cell Biol. 2002; 4:160–164. [PubMed: 11813001]

Gassen NC, Hartmann J, Zschocke J, Stepan J, Hafner K, Zellner A, Kirmeier T, Kollmannsberger L, Wagner KV, Dedic N, Balsevich G, Deussing JM, Kloiber S, Lucae S, Holsboer F, Eder M, Uhr M, Ising M, Schmidt MV, Rein T. Association of FKBP51 with priming of autophagy pathways and mediation of antidepressant treatment response: evidence in cells, mice, and humans. PLoS Med. 2014; 11:e1001755. [PubMed: 25386878]

George JM, Jin H, Woods WS, Clayton DF. Characterization of a novel protein regulated during the critical period for song learning in the zebra finch. Neuron. 1995; 15:361–372. [PubMed: 7646890]

Hay BA, Maile R, Rubin GM. P element insertion-dependent gene activation in the Drosophila eye. Proc Natl Acad Sci USA. 1997; 94:5195–5200. [PubMed: 9144214]

Ibáñez P, Bonnet AM, Débarges B, Lohmann E, Tison F, Pollak P, Agid Y, Dürr A, Brice A. Causal relation between alpha-synuclein gene duplication and familial Parkinson's disease. Lancet. 2004; 364:1169–1171. [PubMed: 15451225]

Iwai A, Masliah E, Yoshimoto M, Ge N, Flanagan L, de Silva HA, Kittel A, Saitoh T. The precursor protein on non-AB component of Alzheimer's disease amyloid is a presynaptic protein of the central nervous system. Neuron. 1995; 14:467–475. [PubMed: 7857654]

Jang SW, Liu X, Chan CB, Weinshenker D, Hall RA, Xiao G, Ye K. Amitriptyline is a TrkA and TrkB receptor agonist that promotes TrkA/TrkB heterodimerization and has potent neurotrophic activity. Chem Biol. 2009; 16:644–656. [PubMed: 19549602]

Kanaan NM, Manfredsson FP. Loss of functional alpha-synuclein: a toxic event in Parkinson's disease? J Parkinsons Dis. 2012; 2:249–267. [PubMed: 23938255]

Kubera M, Holan V, Mathison R, Maes M. The effect of repeated amitriptyline and desipramine administration on cytokine release in C57BL/6 mice. Psychoneuroendocrinol. 2000; 25:785–797.

Lapidus LJ. Understanding protein aggregation from the view of monomer dynamics. Mol BioSyst. 2013; 9:29–35. [PubMed: 23104145]

Lapidus LJ, Eaton WA, Hofrichter J. Dynamics of intramolecular contact formation in polypeptides: distance dependence of quenching rates in a room-temperature glass. Physical Rev Letters. 2001; 87:4.

Lashuel HA, Overk CR, Oueslati A, Masliah E. The many faces of α-synuclein: from structure and toxicity to therapeutic target. Nature Rev Neurosci. 2013; 14:38–48. [PubMed: 23254192]

Liu F, Nguyen JL, Hulleman JD, Li L, Rochet J-C. Mechanisms of DJ-1 neuroprotection in a cellular model of Parkinson's disease. J Neurochem. 2008; 105:2435–2453. [PubMed: 18331584]

Luk KC, Hyde EG, Trojanowski JQ, Lee VM-Y. Sensitive fluorescence polarization technique for rapid screening of alpha-synuclein oligomerization/fibrillization inhibitors. Biochemistry. 2007; 46:12522–12529. [PubMed: 17927212]

Luk KC, Kehm V, Carroll J, Zhang B, O'Brien P, Trojanowski JQ, Lee VM. Pathological alpha-synuclein transmission initiates Parkinson-like neurodegeneration in nontransgenic mice. Science. 2012; 338:949–953. [PubMed: 23161999]

Masliah E, Rockenstein E, Veinbergs I, Mallory M, Hashimoto M, Takeda A, Sagara Y, Sisk A, Mucke L. Dopaminergic loss and inclusion body formation in α-synuclein mice: Implications for neurodegenerative disorders. Science. 2000; 287:1265–1269. [PubMed: 10678833]

McCann H, Stevens CH, Cartwright H, Halliday GM. α-Synucleinopathy phenotypes. Parkinsonism Relat Disord. 2014; 20S1:S62–S67.

McDonald WM, Richard IH, DeLong MR. Prevalence, etiology, and treatment of depression in Parkinson's disease. Biol Psychiat. 2003; 54:363–375. [PubMed: 12893111]

Menza M, Dobkin RD, Marin H, Mark MH, Gara M, Buyske S, Bienfait K, Dicke A. A controlled trial of antidepressants in patients with Parkinson's disease and depression. Neurology. 2009; 72:886–892. [PubMed: 19092112]

Metallo SJ. Intrinsically disordered proteins are potential drug targets. Curr Opin Chem Biol. 2010; 14:481–488. [PubMed: 20598937]

Murphy DD, Rueter SM, Trojanowski JQ, Lee VM. Synucleins are developmentally expressed, and alpha-synuclein regulates the size of the presynaptic vesicular pool in primary hippocampal neurons. J Neurosci. 2000; 20:3214–3220. [PubMed: 10777786]

Nibuya M, Morinobu S, Duman RS. Regulation of BDNF and trkB mRNA in rat brain by chronic electroconvulsive seizure and antidepressant drug treatments. J Neurosci. 1995; 15:7539–7547. [PubMed: 7472505]

Nibuya M, Nestler EJ, Duman RS. Chronic antidepressant administration increases the expression of cAMP response element binding protein (CREB) in rat hippocampus. J Neurosci. 1996; 16:2365–2372. [PubMed: 8601816]

Obuchowicz E, Kowalski J, Labuzek K, Krysiak R, Pendzich J, Herman ZS. Amitriptyline and nortriptyline inhibit interleukin-1β and tumour necrosis factor-α release by rat mixed glial and microglial cell cultures. Int J Neuropsychopharmacol. 2006; 9:27–35. [PubMed: 15963243]

Paumier KL, Luk KC, Manfredsson FP, Kanaan NM, Lipton JW, Collier TJ, Steece-Collier K, Kemp CJ, Celano S, Schulz E, Sandoval IM, Fleming S, Dirr E, Polinski NK, Trojanowski JQ, Lee VM, Sortwell CE. Intrastriatal injection of pre-formed mouse α-synuclein fibrils into rats triggers α-synuclein pathology and bilateral nigrostriatal degeneration. Neurobiol Dis. 2015a; 82:185–199. [PubMed: 26093169]

Paumier KL, Siderowf AD, Auinger P, Oakes D, Madhavan L, Espay AJ, Revilla FJ, Collier TJ. Parkinson Study Group Genetics Epidemiology Working Group. Tricyclic antidepressants delay the need for dopaminergic therapy in early Parkinson's disease. Mov Disord. 2012; 27:880–887. [PubMed: 22555881]

Paumier KL, Sortwell CE, Madhavan L, Terpstra B, Celano SL, Green JJ, Imus NM, Marckini N, Daley B, Steece-Collier K, Collier TJ. Chronic amitriptyline treatment attenuates nigrostriatal degeneration and significantly alters trophic support in a rat model of parkinsonism. Neuropsychopharmacol. 2015b; 40:874–883.

Perez RG, Hastings TG. Could loss of alpha-synuclein function put dopaminergic neurons at risk? J Neurochem. 2004; 89:1318–1324. [PubMed: 15189334]

Pinotsi D, Michel CH, Buell AK, Laine RF, Mahou P, Dobson CM, Kaminski CF, Kaminski Schierle GS. Nanoscopic insights into seeding mechanisms and toxicity of α-synuclein species in neurons. Proc Natl Acad Sci USA. 2016; 113:3815–3819. [PubMed: 26993805]

Polymeropoulos MH, Lavedan C, Leroy E, Ide SE, Dehejia A, Dutra A, Pike B, Root H, Rubenstein J, Boyer R, Stenroos ES, Chandrasekharappa S, Athanassiadou A, Papapetropoulos T, Johnson WG, Lazzarini AM, Duvoisin RC, Di Iorio G, Golbe LI, Nussbaum RL. Mutation in the alpha-synuclein gene identified in families with Parkinson's disease. Science. 1997; 276:2045–2047. [PubMed: 9197268]

Rantamäki T, Vesa L, Antila H, Di Lieto A, Tammela P, Schmitt A, Lesch KP, Rios M, Castrén E. Antidepressant drugs transactivate TrkB neurotrophin receptors in the adult rodent brain independently of BDNF and monoamine transporter blockade. PLoS One. 2011; 6:e20567. [PubMed: 21666748]

Rockenstein E, Mallory M, Hashimoto M, Song D, Shults CW, Lang I, Masliah E. Differential neuropathological alterations in transgenic mice expressing alpha-synuclein from the platelet-derived growth factor and Thy-1 promoters. J Neurosci Res. 2002; 68:568–578. [PubMed: 12111846]

Sadeghi H, Hajhashemi V, Minaiyan M, Movahedian A, Talebi A. A study of the mechanisms involving the anti-inflammatory effect of amitriptyline in carrageenan-induced paw edema in rats. Eur J Pharmacol. 2011; 667:396–401. [PubMed: 21645506]

Sairanen M, O'Leary OF, Knuuttila JE, Castren E. Chronic antidepressant treatment selectively increases expression of plasticity-related proteins in the hippocampus and prefrontal cortex of the rat. Neurosci. 2007; 144:368–374.

Simón-Sánchez J, et al. Genome-wide association study reveals genetic risk underlying Parkinson's disease. Nat Genet. 2009; 41:1308–1312. [PubMed: 19915575]

Singleton AB, et al. alpha-Synuclein locus triplication causes Parkinson's disease. Science. 2003; 302:841. [PubMed: 14593171]

Snead D, Eliezer D. Alpha-synuclein function and dysfunction on cellular membranes. Exp Neurobiol. 2014; 23:292–313. [PubMed: 25548530]

Spillantini MG, Schmidt ML, Lee VM, Trojanowski JQ, Jakes R, Goedert M. Alpha-synuclein in Lewy bodies. Nature. 1997; 388:839–840. [PubMed: 9278044]

Steffan JS, Bodai L, Pallos J, Poelman M, McCampbell A, Apostol BL, Kazantsev A, Schmidt E, Zhu YZ, Greenwald M, Kurokawa R, Housman DE, Jackson GR, Marsh JL, Thompson LM. Histone deacetylase inhibitors arrest polyglutamine-dependent neurodegeneration in Drosophila. Nature. 2001; 413:739–743. [PubMed: 11607033]

Szabo A, Schulten K, Schulten Z. First passage time approach to diffusion controlled reactions. J Chem Phys. 1980; 72:4350–4357.

Theillet FX, Binolfi A, Bekei B, Martorana A, Rose HM, Stuiver M, Verzini S, Lorenz D, van Rossum M, Goldfarb D, Selenko P. Structural disorder of monomeric α-synuclein persists in mammalian cells. Nature. 2016; 530:45–50. [PubMed: 26808899]

Tóth G, et al. Targeting the intrinsically disordered structural ensemble of α-synuclein by small molecules as a potential therapeutic strategy for Parkinson's disease. PLoS ONE. 2014; 9:e87133. [PubMed: 24551051]

Valera E, Masliah E. Combination therapies: the next logical step for the treatment of synucleinopathies? Mov Disord. 2016; 31:225–234. [PubMed: 26388203]

Valera E, Ubhi K, Mante M, Rockenstein E, Masliah E. Antidepressants reduce neuroinflammatory responses and astroglial alpha-synuclein accumulation in a transgenic mouse model of multiple system atrophy. Glia. 2014; 62:317–337. [PubMed: 24310907]

Volpicelli-Daley LA, Luk KC, Patel TP, Tanik SA, Riddle DM, Stieber A, Meaney DF, Trojanowski JQ, Lee VM. Exogenous α-synuclein fibrils induce Lewy body pathology leading to synaptic dysfunction and neuron death. Neuron. 2011; 72:57–71. [PubMed: 21982369]

Watson JB, Hatami A, David H, Masliah E, Roberts K, Evans CE, Levine MS. Alterations in corticostriatal plasticity in mice overexpressing human alpha-synuclein. Neuroscience. 2009; 159:501–513. [PubMed: 19361478]

Winner B, Jappelli R, Maji SK, Desplats PA, Boyer L, Aigner S, Hetzer C, Loher T, Viular M, Campioni S, Tzitzilonis C, Soragni A, Jessberger S, Mira H, Consiglio A, Pham E, Masliah E, Gage FH, Riek R. In vivo demonstration that α-synuclein oligomers are toxic. Proc Natl Acad Sci USA. 2011; 108:4194–4199. [PubMed: 21325059]

Xu H, Steven Richardson J, Li XM. Dose-related effects of chronic antidepressants on neuroprotective proteins BDNF, Bcl-2 and Cu/Zn-SOD in rat hippocampus. Neuropsychopharmacol. 2003; 28:53–62.

Yu S, Li X, Liu G, Han J, Zhang C, Li Y, Xu S, Liu C, Gao Y, Yang H, Uéda K, Chan P. Extensive nuclear localization of alpha-synuclein in normal rat brain neurons revealed by a novel monoclonal antibody. Neuroscience. 2007; 145:539–555. [PubMed: 17275196]

Zhu M, De Simone A, Schenk D, Toth G, Dobson CM, Vendruscolo M. Identification of small-molecule binding pockets in the soluble monomeric form of the AB42 peptide. J Chem Phys. 2013; 139:035101. [PubMed: 23883055]

Zschocke J, Rein T. Antidepressants encounter autophagy in neural cells. Autophagy. 2011; 7:1247–1248. [PubMed: 21642768]

Highlight

- Nortriptyline inhibits aggregation of alpha-synuclein in cell and animal models.
- Nortriptyline enhances molecular reconfiguration to inhibit aggregation.
- Nortriptyline has disease-modifying potential for treatment of synucleinopathies.

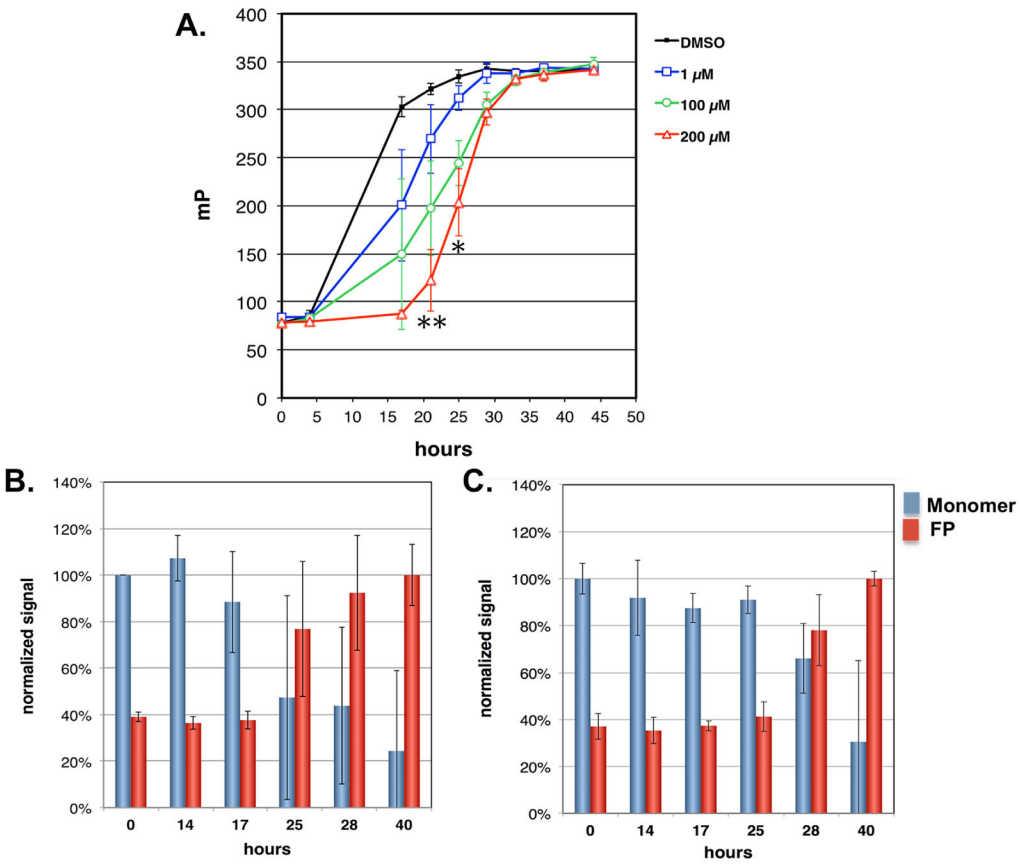

Figure 1. Nortriptyline delays initiation of α-syn aggregation and conversion of α-syn monomer to higher molecular weight species

A) Aggregation of recombinant α-syn (70μM) in the presence of DMSO (black), 1μM (blue), 100μM (green), and 200μM (red) NOR was induced by gentle agitation at 37°C. Introduction of NOR was associated with a dose-related delay in α-syn aggregation as measured by fluorescence polarization. Fluorescence polarization is expressed in millipolarization (mP) units. Each time point is expressed as mean ± SD. NOR treatment groups were compared to DMSO-only group with two-tailed t-test, *$p<0.05$, **$p<0.01$. B&C) Recombinant α-syn (70μM) was incubated with gentle agitation in the presence of vehicle (B) or 100μM NOR (C). Aliquots were removed at the indicated times and average molecular size determined by fluorescence polarization of Alexafluor 594 α-syn conjugate tracer (red bars) and the amount of monomeric α-syn determined by size exclusion (blue bars). Monomer was normalized to reading at 0 hours for each tube. Fluorescence polarization was normalized to reading at 40 h for each tube. In both conditions, increased fluorescence polarization coincided with loss of monomer and NOR delayed this conversion to higher molecular weight species. Values are expressed as mean +/− SD.

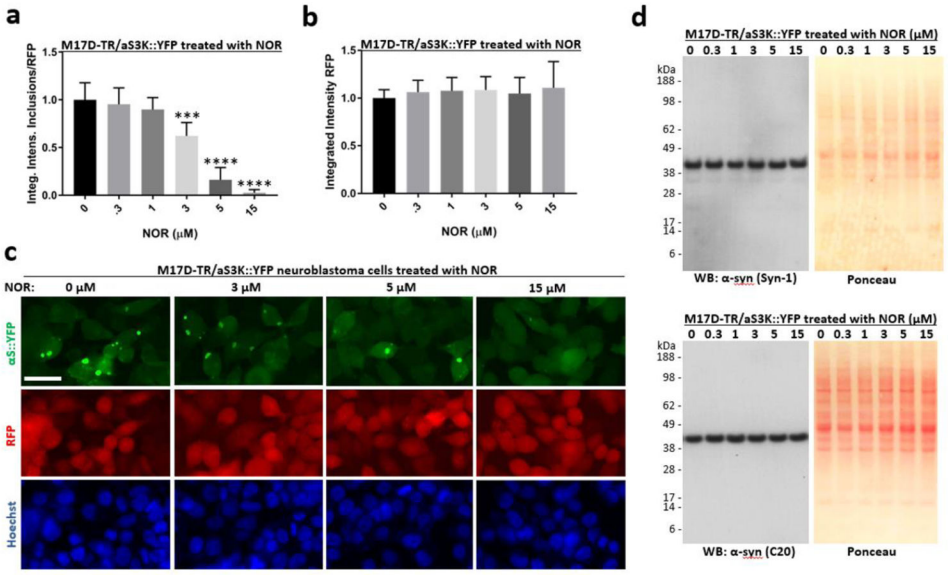

Figure 2. Nortriptyline reduces inclusion formation in M17D neuroblastoma cells that express inclusion-prone αS3K::YFP

A) M17D cells that express an αS-3K::YFP fusion protein (dox-inducible) and RFP (constitutive) were treated with NOR at 0 (= DMSO alone at 0.1% f.c.), 0.3, 1, 3, 5 and 15 μM. αS-3K::YFP expression was induced at the same time point and IncuCyte-based analysis of punctate YFP signals relative to total RFP was performed 24 h later. YFP inclusion integrated intensities and RFP total integrated intensities were measured and the ratio was calculated. Four independent experiments (N = 4, n = 12), the data are presented as mean ± SD. ***p<0.001, ****p<0.0001 versus 0 μM NOR (whose mean was set to 1 in each experiment), repeated-measures one-way ANOVA followed by Dunnett's multiple comparisons *post hoc* test. B) Same as A, but only the total integrated intensities of co-expressed RFP are plotted. No significant changes were observed. C) Representative images (YFP, RFP and Hoechst staining) for the indicated NOR concentrations; scale bar = 20μm. D) Western blots using α-syn-specific mAb Syn-1 and pAb C20, plus Ponceau-stained membranes.

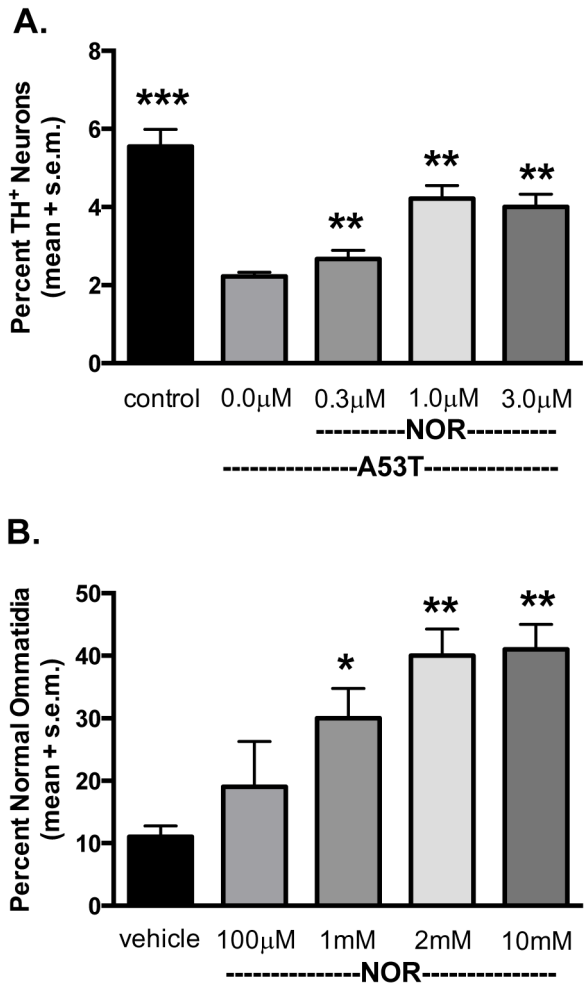

Figure 3. Nortriptyline attenuates neurotoxicity elicited by A53T α-syn in a primary cell culture model and α-syn-induced retinal degeneration in transgenic *Drosophila*

A) Primary midbrain cultures were untreated ('control') or transduced with A53T α-syn lentivirus in the absence or presence of NOR. The cells were stained with antibodies specific for MAP2 and TH and scored for dopaminergic cell viability (%MAP2+/TH+). The data are presented as the mean ± SEM. $^{**}p<0.01$, $^{***}p<0.005$ versus A53T, square root transformation, repeated-measures, one-way ANOVA followed by Tukey's multiple comparisons *post hoc* test. B) Transgenic *Drosophila* less than 12 hours after hatching were transferred to vials with food hydrated with either water or an aqueous solution of NOR at the indicated concentrations. After 7 days, retinas were assessed by the pseudopupil assay. Data are presented as mean +/− SEM and analyzed by one-way ANOVA followed by Dunnett's multiple comparison *post hoc* test. $^{*}p \leq 0.05$, $^{**}p \leq 0.01$.

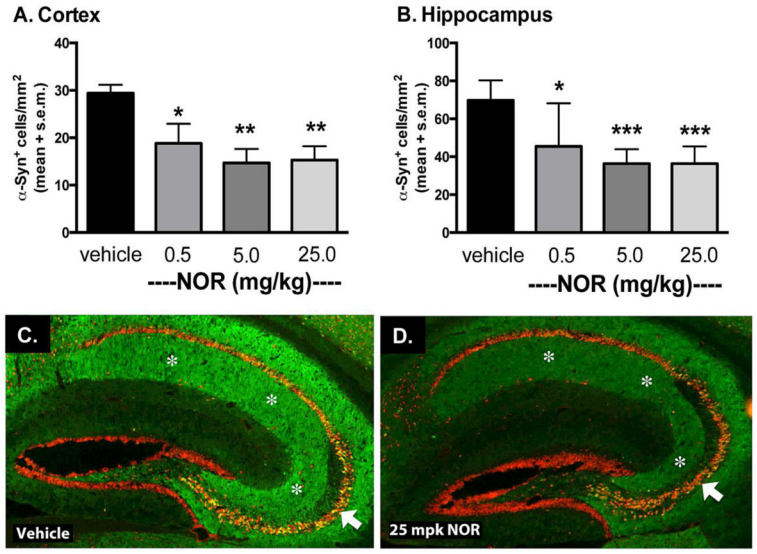

Figure 4. Nortriptyline reduces accumulation of human α-syn in transgenic mice

Six-month-old mice were treated for 30 days with vehicle (N=7), 0.5 mg/kg (N=6), 5 mg/kg (N=6), or 25 mg/kg (N=7) NOR. Treatment with NOR reduced the number of cells immunoreactive for human α-syn in both **A.** cortex and **B**. hippocampus. **C & D.** Representative sections from the hippocampus show reduced α-syn accumulation (green) in cell bodies and the neuropil without affecting neuronal architecture as judged by NeuN immunostaining (red). White arrows indicate hippocampal pyramidal cell layer; white asterisks indicate hippocampal neuropil. Data represent mean ± SEM. Statistical significance determined by one-way ANOVA with Dunnett's *post hoc* test. *$p \leq 0.05$, **$p \leq 0.01$, *** $p \leq 0.001$.

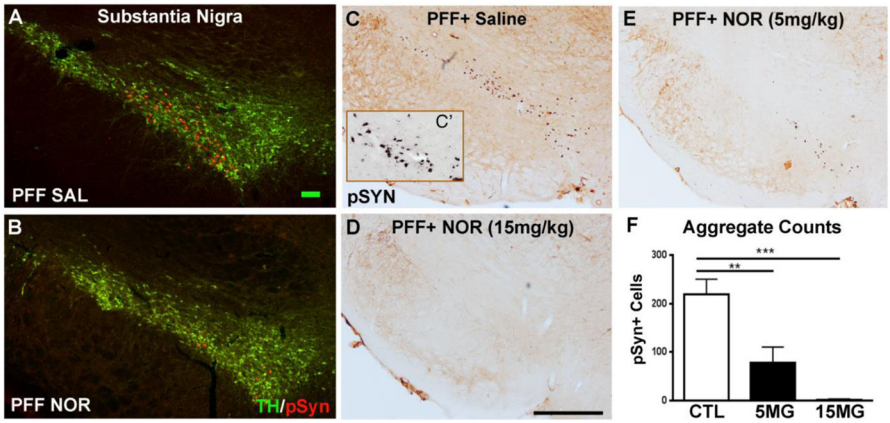

Figure 5. Nortriptyline pre-treatment reduces the number of α-syn aggregates in substantia nigra in the rat PFF model

A&B: dual label fluorescence immunocytochemistry for tyrosine hydroxylase (TH, green) and S129 phosphorylated α-syn (pSyn, red) illustrating reduced formation of α-syn aggregates in substantia nigra dopamine neurons with NOR treatment. C–E: light microscopy of pSyn aggregates (brown) showing dose-related reduction with NOR. C′: pSyn aggregates following proteinase K digestion confirming their identity as aggregates of insoluble α-syn. F: counts of pSyn aggregates in SN with increasing doses of NOR: vehicle (N=6), NOR (5mg/kg)(N=6), NOR (15mg/kg)(N=6). Treatment effect ($F(2,11)=20.38$; $p=0.0002$) for total counts of pSyn-positive aggregates. Post-hoc tests indicate that both the low (**$p<0.01$) and high dose (***$p<0.001$) NOR-treated rats had significantly fewer aggregates in SN as compared to saline treated animals.

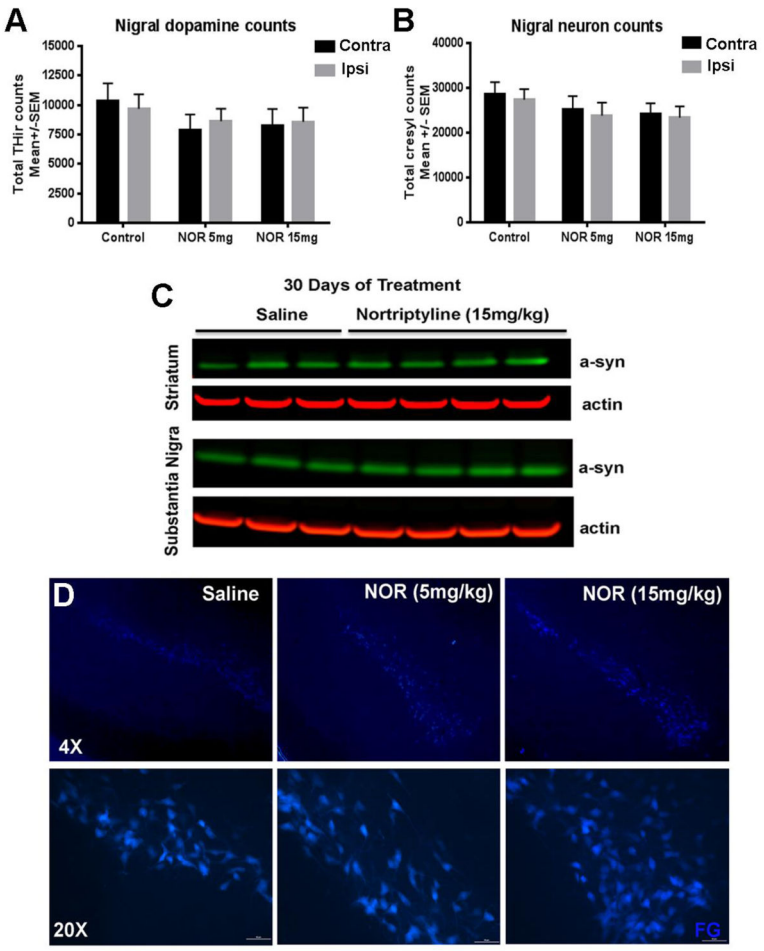

Figure 6. Nortriptyline-mediated reduction of pathology in the PFF rat model is not due to neuron loss, reduced levels of endogenous alpha-synuclein, or inhibition of retrograde transport

A–B) Stereological counts of TH+ and cresyl violet stained substantia nigra neurons indicate that the reduction in pathology was not due to frank loss of DA neurons with NOR treatment. In the legend, “Contra” refers to the hemisphere contralateral to PFF injection and “”Ipsi” refers to the hemisphere ipsilateral to PFF injection. C) Western blots show that levels of endogenous α-syn in the striatum and substantia nigra after 30 days of daily NOR treatment remain unchanged compared to saline treatment.. D) Fluorescence micrographs of substantia nigra show no difference in fluorogold transport between groups, consistent with no impairment of retrograde transport with NOR treatment.

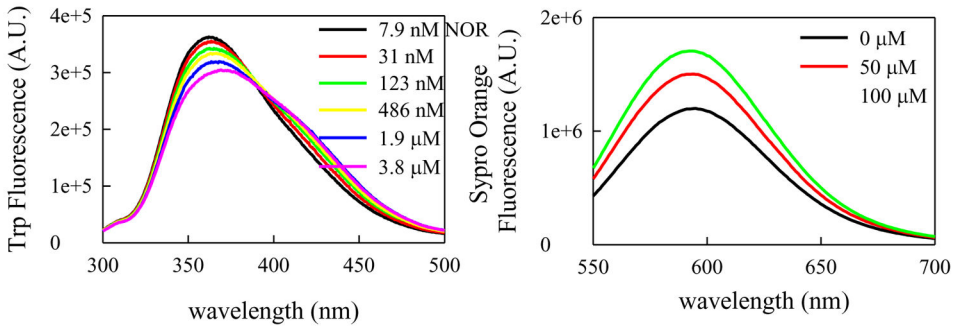

Figure 7. Nortriptyline interacts with monomeric α-syn to inhibit a compact conformation

A) Fluorescence of W94 with increasing [NOR]. The red shift suggests W94 is more solvent exposed when bound to NOR. B) Fluorescence of Sypro Orange with α-syn with increasing [NOR]. Increased fluorescence indicates increased exposure of hydrophobic residues.

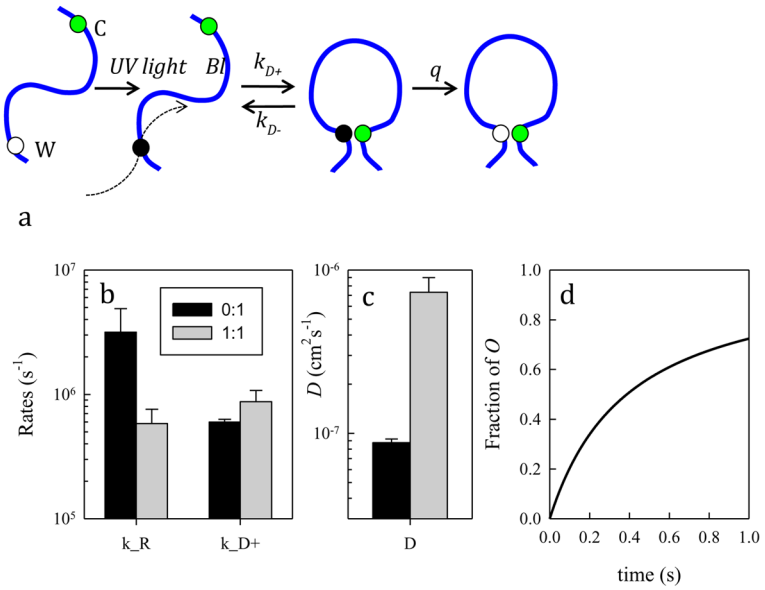

Figure 8. Trp-Cys contact quenching indicates that in the presence of nortriptyline, the α-syn chain is less compact, more labile and less prone to forming oligomers

a) Schematic for the determination of the rate of contact formation between the probe, tryptophan (W), and the quencher, cysteine (C), within an unfolded protein. Pulsed optical excitation leads to population of the lowest excited triplet state of tryptophan. Tryptophan contacts cysteine in a diffusion-limited process with rate k_{D+}, and then either diffuses away (k_{D-}) or is quenched (q) by the cysteine. b) Reaction-limited and diffusion-limited rates for α-syn without (black) and with (gray) equimolar NOR at 30°C. c) Intramolecular diffusion coefficients calculated at 30°C with the same colors as (b). d) Calculated formation of O (α-syn oligomers), from scheme “i” in the text, for rates describing the protein without (black) and with NOR (gray).